# Inherently Charged Particle (ICP) Sensor Design

Laura Salo, Antti Rostedt, Heino Kuuluvainen, Kimmo Teinilä, Rakesh K. Hooda, Md. Hafizur Rahman, Arindam Datta, Ved Prakash Sharma, Sanjukta Subudhi, Antti Hyvärinen, Hilkka Timonen, Eija Asmi, Sampsa Martikainen, Panu Karjalainen, Banwari Lal, Jorma Keskinen, and Topi Rönkkö

***Abstract*—Ambient particles from natural and anthropogenic sources are a major cause of premature deaths globally. While there are many instruments suitable for scientific measurements of aerosols, better methods for long-term monitoring purposes are still needed, especially low-maintenance, affordable solutions for ultrafine particles. In this article, we present a new sensor design and prototype, the inherently charged particle (ICP) sensor, which uses the preexisting electrical charge of particles to measure particle concentration, instead of employing a charging mechanism, as is typical for instruments based on electrical detection. When the ICP-sensor is employed in conjunction with another instrument, information on the particle charge state can also be derived. We present the results of a laboratory characterization as well as two measurements in suggested applications: 1) engine exhaust measurements and 2) ambient measurements in a traffic environment, where we compare the sensor response to three particle concentration metrics: 1) number; 2) surface area; and 3) mass. The sensor proved suitable for both applications, the signal correlated best with number concentration in the engine emission measurements and with particle surface area in the ambient measurements. The measured charge concentrations were well-correlated ($R^2 > 0.8$) with theoretical values calculated from the number size distribution assuming an equilibrium charge distribution.**

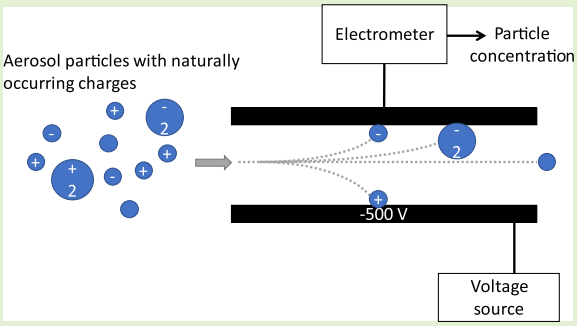


***Index Terms*—Air pollution, air quality monitoring, ultrafine particles.**

## I. Introduction

PARTICLES in the air are known to contribute to cloud formation and atmospheric radiative forcing [1], [2] and they have adverse effects on human health [3]. High particle pollution levels are a problem, especially in large cities, as cities bring together particle sources (traffic and heating) and large numbers of people. The risk of major wildfires is also growing with the increased temperature due to changes in land use and global warming [4]. The World Health Organization (WHO) has set targets for particle concentration levels and air quality monitoring is key in making sure that those targets are met. In addition to well-equipped monitoring stations with a variety of gaseous and particle measurement instruments, sensor-type monitoring is needed for a denser measurement network. Long-term monitoring with sensor networks can expose particle sources and show particle dispersion patterns. In addition, sensor data are used to inform air quality modeling, e.g., The Finnish Meteorological Institute's ENvironmental information FUsion SERvice (FMI-ENFUSER), which is used to show real time and predicted urban air quality (https://en.ilmatieteenlaitos.fi/environmental-information-fusion-service).

Different types of particle sensors give different information. For example, the most common and inexpensive solutions rely on optical detection of particles sized ~0.3 $\mu$m and larger–smaller particles cannot be detected because their size is close to the wavelength of light [5]. Optical measurement gives a signal that correlates with the mass concentration of particles. Some optical sensors target specific compounds such as black carbon (BC); these sensors operate by collecting particles on a filter and measuring the attenuation of light through the filter [6]. Electrical measurement of diffusion-charged (DC) particles can detect much smaller particles, down to approximately 10 nm, and the signal of DC particles

Manuscript received 26 October 2022; revised 14 December 2022; accepted 19 December 2022. Date of publication 4 January 2023; date of current version 13 February 2023. This work was supported in part by the Business Finland and the Department of Biotechnology, India, through the Project "Traffic and Air Quality in India: Technologies and Attitudes (TAQIITA)" as well as companies Neste, Dekati, Pegasor, and Helsinki Region Environmental Services Authority (HSY), under Grant 2763/31/2015; and in part by the Academy of Finland Flagship: The Atmosphere and Climate Competence Center (ACCC) through Tampere University under Grant 337551 and through the Finnish Meteorological Institute under Grant 337552. The work of Laura Salo was supported by the Doctoral School of Tampere University of Technology (now Tampere University). The associate editor coordinating the review of this article and approving it for publication was Prof. Stefan J. Rupitsch. *(Corresponding author: Laura Salo.)*

Laura Salo, Antti Rostedt, Heino Kuuluvainen, Sampsa Martikainen, Panu Karjalainen, Jorma Keskinen, and Topi Rönkkö are with the Aerosol Physics Laboratory, Tampere University, 33720 Tampere, Finland (e-mail: laura.salo@tuni.fi).

Kimmo Teinilä, Rakesh K. Hooda, Antti Hyvärinen, Hilkka Timonen, and Eija Asmi are with the Aerosol Composition Research Group, Finnish Meteorological Institute, 00560 Helsinki, Finland.

Md. Hafizur Rahman, Arindam Datta, Ved Prakash Sharma, Sanjukta Subudhi, and Banwari Lal are with The Energy and Resources Institute, New Delhi 110003, India.

This article has supplementary downloadable material available at https://doi.org/10.1109/JSEN.2022.3232509, provided by the authors.

Digital Object Identifier 10.1109/JSEN.2022.3232509

is closely correlated with the lung-deposited surface area (LDSA) [7], [8]. To get a full picture of an aerosol population, many particle sizes and metrics must be covered.

Because aerosol particles are small, the electrostatic forces affecting them can be much stronger than the gravitational force [9]. This property is used in many aerosol applications, for example, to remove unwanted particles from a flow with an electrical field or to classify them by size, as in the differential mobility analyzer (DMA), where particles are selected based on their electrical mobility (charge to diameter ratio). Electrical particle sensors do not (usually) rely on the preexisting charge, but instead charge particles by ionizing the surrounding air. A common method is diffusion charging, where particles pass through a chamber with a high-voltage corona needle creating ions. The ions attach to the particle surfaces mainly through movement caused by diffusion [9]. Diffusion charging is employed in many existing commercial particle sensors: 1) nanoparticle surface area monitor (NSAM) (TSI); 2) Partector (Naneos); and 3) AQ Urban (Pegasor), for instance. There are also some examples of sensors employing bipolar charging methods, for example, with a radioactive source [10], [11]. While particles are usually intentionally charged in aerosol instruments based on particle electrical detection, Bilby et al. [12] presented a particle emission sensor utilizing the existing charge on the particles in the engine exhaust. This design, however, is based on the current amplification effect caused by the fragmentation of the collected conductive soot particles inside the sensor. To differentiate between particles charged intentionally for detection or classification and particles charged naturally, the latter will be referred to as indigenously or inherently charged (IC) hereafter. This terminology is also used by Eastwood [13].

In our study, we present a prototype of a new electrical particle sensor, the IC particle (ICP)-sensor, which relies on the IC of particles in the atmosphere or in exhaust. Our study shows that IC can easily be used to monitor particle concentrations, thus removing the necessity of a diffusion charger, at least for some applications. We share our results from two test measurements, first in an engine laboratory where we measured the (diluted) emissions of a heavy-duty truck and second from ambient measurements in a roadside environment with heavy air pollution. We also compare the measured charge concentrations to number, surface area, and mass concentrations of particles as well as theoretical charge concentrations calculated from the particle number distribution.

## II. Theoretical Background

Particle charge is the net charge of all electrons and protons contained in a particle. The number of elementary charges is often reported instead of the absolute charge. Negatively charged particles have more electrons than protons and vice versa. In equilibrium conditions, the charge distribution of particles depends on the ambient temperature, as well as the size of the particles [14]. The equilibrium ambient particle charge distribution can be calculated based on Fuchs' limiting-sphere theory, most conveniently using the formulation by Wiedensohler [15]. The net charge of an ambient particle population is close to zero, but negatively charged particles are slightly more common [16]. The charge distribution of freshly emitted combustion-originated particles is indicative of the temperature when the particles were formed and tend to follow a Boltzmann distribution, although the emitted particles will eventually neutralize to the ambient charge distribution [17], [18]. The time it takes aerosol particles to reach an equilibrium state depends on the availability of gaseous ions, and how far from equilibrium the aerosol population is to begin with. Ambient ion concentrations are typically around $10^3$ ions/cm$^3$ [16], but polluted air tends to have fewer ions, as they either grow into larger ions (particles) or are scavenged by existing particles [19]. Jayaratne et al. [20] showed that cluster ions near a road were rapidly scavenged by particles, but highly charged particles were detected up to 400 m from the road, giving some indication of the timeframe it takes for particles to reach an equilibrium charge distribution.

Previous studies have shown ways in which the particle charge of IC particles can be used to understand particle sources. Burtscher et al. [17] showed that particles produced by combustion had charge distributions, which could be related back to the process that created the particles. Kittelson and Pui [21] studied the charged fraction of particles (by mass) from exhaust and found a range of 72% during idle to 88% at full load. They also measured the charge distribution by electrical mobility and found that there were equal amounts of positive and negative particles. Maricq [18] also measured particle charge distributions from a motor vehicle and determined that the distributions corresponded to Boltzmann distributions at temperatures of 800–1100 K. Like Kittelson and Pui, he also found there to be equal amounts of positive and negative charges. In addition, Lähde et al. [22] reported on the ion number concentration distribution in heavy-duty diesel engine exhaust, finding that far fewer ions were present in the exhaust when using a diesel particulate filter (DPF), compared to no after treatment, or a diesel oxidation catalyst (DOC). Large amounts of charged particles (ions) have also been observed when measuring near busy roads [20], [23], [24] and the number of charges carried by ultrafine particles has been found to be larger near traffic than in background locations [24] or near powerlines [23]. Other types of combustion also produce charged particles, for example, natural gas engines [25], mixed pulverized coal and wood pellets in power plant boilers [26], and cooking on a gas stove [27].

Fig. 1 shows the average number of charges per particle for 10-nm-to-1-$\mu$m particles at temperatures of 20 °C–1000 °C. Even at high temperatures, many particles are neutral, which is why the average number of charges can remain below one. The black line represents a typical diffusion charger, this one is the electrical low-pressure impactor (ELPI+, Dekati Ltd.) $Pn$-curve [28], and the other lines show how temperature affects the charge distribution. A $Pn$-curve describes the efficiency of a charger, giving the average charge per particle as a function of particle size. Diffusion charging imparts a much higher charge to the particles than they would have otherwise.

The Boltzmann charge distribution is symmetrical around 0, i.e., the number of charges is the same for negative and positive charges, and therefore, only one line is shown in Fig. 1

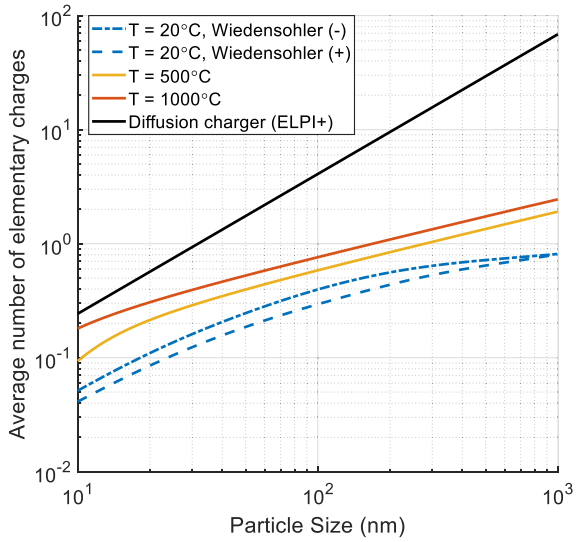


Fig. 1. Boltzmann equilibrium mean particle charge as a function of particle size at two different temperatures, as well as the Wiedensohler mean charge at $T = 20$ °C. The *Pn* curve of the ELPI+ charger is also shown (black line).

for each temperature (the other line can be imagined to be on top). The Wiedensohler distribution charge distribution is more accurate at ambient temperatures, especially at the lower particle sizes where the Boltzmann distribution underestimates the mean charge [15]. Unlike the Boltzmann distribution, it is not symmetrical, and thus, both the negative and positive charge numbers are shown. Later in this article, we will use the Wiedensohler distribution for the negative charge fraction when comparing our measurements to a theoretical ambient charge distribution and the Boltzmann distributions when comparing exhaust aerosol measurements

## III. Sensor Design

For our sensor design, we used a zeroth-order mobility analyzer, or electrostatic collector, with annular geometry. A cross-sectional drawing of the mobility analyzer is shown in Fig. S1. The inner electrode is connected to a voltage source and the outer electrode is connected to an electrometer. The basic principle of any mobility analyzer is that particles travel through an electric field, and particles with a high enough electrical mobility $Z$ are collected, while low mobility particles travel through. This type of an analyzer can be characterized by the smallest electrical mobility ($Z_0$) that has a 100% collection efficiency [29], and for an annular geometry, it is given by (1), where $Q$ is the volumetric air flow rate, $d_{\text{outer}}$ and $d_{\text{inner}}$ are the diameters of the electrodes, $L$ is their length, and $V$ is the voltage difference across the electrodes. The ratio of a particle's mobility to the limiting mobility is the collection efficiency $\eta$ (2) when the flow is laminar

$$Z_0 = \frac{Q \ln\left(\frac{d_{\text{outer}}}{d_{\text{inner}}}\right)}{2\pi L V} \tag{1}$$

$$\eta = \frac{Z}{Z_0}. \tag{2}$$

The electrical mobility of a particle is given by (3), where $n$ is the number of elementary charges, $e$ is equal to one elementary charge ($1.602 \times 10^{-19}$ $C$), $C(d_p)$ is the Cunningham slip correction factor, $\eta(T)$ is the viscosity of the surrounding gas, dependent on the gas temperature $T$, and $d_p$ is the particle diameter. As can be seen from the equation, particles have high electrical mobility if they are small and highly charged. Ignoring the slip correction, a singly charged particle has the same mobility as a twice charged particle of double the diameter (including the slip correction would increase the mobility of the smaller particle compared to the larger)

$$Z = \frac{neC\left(d_p\right)}{3\pi\,\eta\left(T\right)d_p}. \tag{3}$$

TABLE I
Important Dimensions and Other Parameters of the Sensor

| Parameter | Value |
|---|---|
| $L$ | 48 mm |
| $L_{outer}$ | 50 mm |
| $d_{outer}$ | 32 mm |
| $d_{inner}$ | 28 mm |
| $Q$ | 1 Lpm |
| $V$ | ±500 V |
| $Z_0$ | $1.466\times10^{-4}$ cm$^2$/(V·s) |

The dimensions and other constant parameters used in our sensor are shown in Table I. The measurement electrode was slightly longer than the opposing high-voltage electrode to minimize particle losses caused by the edge effects of the electric field. The $L$ value shown and used for calculation is for the shorter electrode.

The $Z_0$ value above corresponds to a singly charged particle with a diameter of 140 nm or a doubly charged particle with a diameter of 220 nm, which is suitable for measuring most urban particles or engine emitted particles. The same sensor geometry can easily be changed to target various mobility sizes, either by changing the flow rate or the collection voltage. When characterizing the sensor efficiency, we also used lower voltages to change the $Z_0$ value.

In addition to the mobility analyzer, the ICP-sensor consisted of an ion trap to prevent the measurement of gaseous ions; a voltage source, electrometer, and computer connected to the mobility analyzer; a critical orifice to control the flow rate; and a pump. In the engine laboratory and ambient measurements, we also used a cyclone to prevent coarse dust from entering the sensor.

## IV. Methods

We measured the sensor's detection efficiency dependency on particle mobility, size, and number concentration in a laboratory. We then tested the ICP-sensor for two applications: measuring particles from engine exhaust from a heavy-duty truck as well as ambient aerosol in an urban traffic environment. Correlations with different metrics were calculated using simple linear regression with ordinary least squares method.

### A. Laboratory Measurement of Detection Efficiency

The laboratory characterization was conducted at the Tampere University Aerosol Physics Calibration Laboratory.

To measure the detection efficiency of the ICP-sensor, we built the setup shown in Fig. S2 and used the singly charged aerosol reference (SCAR) system to produce a monodisperse aerosol of unipolar, singly charged particles [30]. Our main reference for the detection efficiency was a Faraday cup and electrometer (FCAE) (Keithley 6430 Sub-femtoamp Remote Sourcemeter, Keithley Inc.), FCAE. In addition, particles penetrating through the sensor were measured with a condensation particle counter (CPC 3750, by TSI).

For the most part, only the mobility analyzer portion of the ICP was characterized, but we also conducted a few measurement points with the ion trap in place, in order to characterize the losses in the ion trap for small particles.

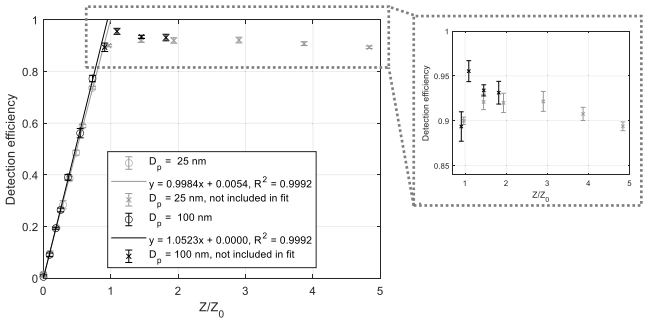


Fig. 2. Detection efficiency of the sensor prototype as a function of particles' electrical mobility divided by the minimum electrical mobility. The variation in the ratio $Z/Z_0(V)$ was achieved by varying the collection voltage. Two particle sizes were used, 25 and 100 nm.

### B. Engine Laboratory Measurements

The engine laboratory measurements were conducted at Indian Oil Corporation (IOCL) facilities in Faridabad, using a chassis dynamometer. The test subject was a typical Indian heavy-duty truck, registered in 2017 and equipped with a DOC, but DPF, and it was driven following a transient driving cycle. The exhaust sampling was conducted using a constant volume sampler (CVS), and we alternated between measuring all particles and solid particles. A thermodenuder was used to remove the semivolatile particle fraction in the latter case, as shown in the simple schematic (Fig. S3). The measurement matrix included three different fuels and two lubricating oils. The three fuels were Bharat Stage VI (BSVI) fossil fuel, and two fuels blended with Bharat Stage IV (BSIV): 1) renewable paraffinic diesel (RPD) and renewable fatty acid Methyl Esther (r-FAME). The test cycle was the Delhi Bus Driving Cycle, which includes accelerations, decelerations, and idling. One cycle lasts 7 min, and the maximum speed is 50 km/h. For two fuels, the "All particles" measurements were conducted twice, and we were able to measure both the positively and negatively charged particle fractions by changing the collection voltage from +500 to −500 V. The measurement matrix is included in Table S1. Results from the measurement campaign have been previously published [31], and more details on the vehicle, fuels, oils, driving cycle, and so on can be found there.

We used an ELPI+ [28], [32] to measure the particle number and size distribution as well as to compare the ICP to. ELPI+ is a cascade impactor, where each impactor stage is separately connected to an electrometer. The particles are positively charged using diffusion charging. The particles going through the ICP-sensor were measured with an eFilter (by Dekati Ltd., presented in [33]), which also employs diffusion charging. eFilter also allows for collecting particles onto a filter, which can then be weighed to interpret the mass concentration of the sample, but we only used the electrical portion of the instrument. The data output of the instrument is simply the current measured from the DC particles. The sample dilution was calculated using $CO_2$ as a tracer gas.

### C. Ambient Air Measurements on a Roadside

The ambient measurements were conducted in Gual Pahari, located south of New Delhi, in December 2018. During the measurements, the days were sunny, there was almost no wind (<1 m/s), and the temperature ranged between 10 °C and 25 °C. The instruments were housed in a mobile laboratory parked adjacent to a busy road with approximately 800 vehicles per hour during daytime. Fig. S4 shows a simplified schematic of the measurement setup. All instruments sampled air through a PM2.5 inlet, and the ICP had an additional cyclone to prevent the accumulation of coarse dust. The cutoff diameter ($d_{50}$) of the cyclone was 2.239 $\mu$m. The sensor collection voltage was set to −500 V; thus, the measured particles were also negatively charged. Again, ELPI+ was used for comparison and to calculate the theoretical charge concentration. The ELPI+ sample was diluted with 5 L/min of clean air to lessen the accumulation of particles. The total flow for the ELPI+ is 10 L/min, and thus, the dilution ratio was 2 (results corrected to represent ambient concentrations in the data analysis). The measurements are described in more detail in a previous article [34].

## V. Results

In this section, we present the results from each measurement separately, and the three experiments are interpreted together in Section VI.

### A. Mobility Analyzer Characterization

We determined the detection efficiency for the mobility analyzer portion of the ICP by employing (2) for two different particle sizes, 25 and 100 nm, and varied the $Z/Z_0$ ratio by changing the collection voltage of the analyzer.

Fig. 2 shows the detection efficiency of the ICP-sensor as a function of electrical mobility ratio. The ratio $Z/Z_0$ was changed by changing the voltage used to collect particles, $V$ in (1). Ideally, the relationship between detection efficiency and the mobility ratio should be one-to-one, as shown in (2), and the measurements show that this is the case. The fit for 100-nm particles is slightly steeper than the fit for 25-nm particles, due to greater diffusional and electrical losses for the smaller particles. The results for mobility ratios greater than one show that the detection efficiency begins to go down. This is most likely due to the increased electrical field causing losses in the area before the detection plates. We also measured the detection efficiency for the whole sensor (including an ion trap and additional tubing to connect it to the analyzer) in

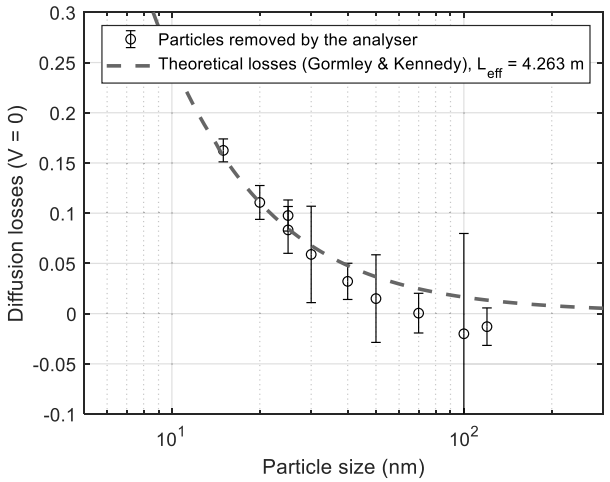


Fig. 3. Particles lost due to diffusion as a function of particle size. Collection voltage $V$ was set to 0 V. The error bars represent the standard deviation of measured variables combined into a total standard deviation using error propagation. The fit line represents theoretical diffusion losses for a tube of length 4.263 m ($L_{\text{eff}}$).

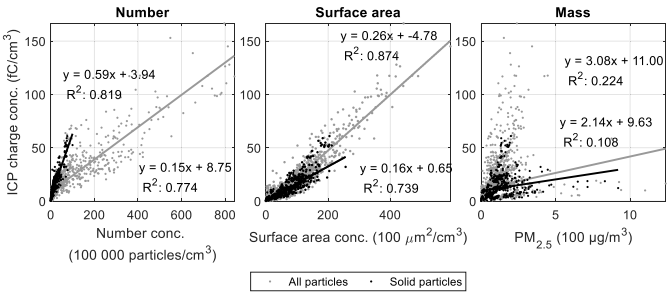


Fig. 4. Charge concentration measured with ICP compared to particle number and mass concentrations during the engine laboratory measurement campaign. These values are corrected for dilution and losses in the thermodenuder, representing the concentrations in the CVS. Each data point is a 5-s average.

a similar measurement but changed particle size (instead of the collection voltage) to vary the mobility ratio (see Fig. S5). As expected, the detection efficiency was slightly lower due to additional diffusion losses (fit line $y = 0.8976\text{x} + 0.0582$ and $R^2 = 0.9988$). Here, we also observed that the detection efficiency began to decrease when $Z/Z_0$ increased past one, due to the increased diffusion losses of smaller particles.

Fig. 3 shows the particle losses due to diffusion in the mobility analyzer inlet, outlet, and annular flow geometry before and after the electrodes. Particles deposited onto the detection cylinder were not counted as losses, i.e., the measured values were calculated as

$$\text{diffusion losses} = 1 - \frac{\text{penetrating particles} + \text{detected particles}}{\text{total concentration}}.$$

The $d_{50}$ value for the lower limit of the mobility analyzer is 5.5 nm, but in practice, the $d_{50}$ size will be larger, and the overall losses greater, as diffusion losses due to the ion trap and tubing are not accounted for here. To compare to a theoretical value, we used Gormley and Kennedy's equation for diffusion losses in a tube [35], calculating the effective length to best match the measured values. We used the form given by Cheng [36]. The diffusion losses for a tube resulted in a good fit, with an effective length of 4.26 m, and this equation is used to correct the theoretical current from the ELPI+ number size distribution. An even better fit might have been achieved by dividing the mobility analyzer into regions and using a combination of equations; however, we preferred this approach due to its simplicity.

Fig. S6 shows the effect of particle concentration on detection efficiency. In theory, high particle number could lower the detection efficiency due to space charge losses. The space charge is caused by our test aerosol, in which all particles are either positively or negatively charged (in this test, they were negatively charged). Consequently, the particles repel each other, and if the particle concentration is large enough, particles may be lost inside the sensor due to movement caused by the space charge. However, we calculated an approximate value for space charge losses inside the sensor, and even with a concentration of $10^7$ particles/cm$^3$, the space charge losses were less than 0.5%. Thus, it is unlikely that the lowering detection efficiency seen in Fig. S6 has to do with this effect. In addition, the space charge losses should continue to reduce detection efficiency with increasing particle concentration, whereas in our results, the detection efficiency levels off at 10 000 particles/cm$^3$, settling at approximately 0.93. In the previous results for detection efficiency, particle concentrations were between 10 and 15 $\times$ $10^3$ particles/cm$^3$ and thus in the level area.

### B. Engine Laboratory Measurements

The engine exhaust particles were small but numerous. Based on the data measured by ELPI+, the count median diameters (CMDs) of the particles were below 30 nm in all cases and the measured number concentration of particles ranged from 50 000 to 800 000 particles/cm$^3$ (after dilution). The median current measured by the ICP ranged from 20 to 70 fA, depending mostly on the phase of the driving cycle. Median values for each measurement point are shown in Table S2 and the particle size distributions of the exhaust sample are presented in Fig. S7. There was no statistical difference between the charge concentrations of different fuels and oils and the in-group variation was large, i.e., if a difference exists, the sample size would need to be larger.

Fig. 4 shows the correlation of the charge concentration to three different particle metrics: 1) number; 2) geometric surface area; and 3) mass ($PM_{2.5}$, mass concentration of sub 2.5 $\mu$m particles). Number, surface area, and mass were chosen for comparison because they are common metrics for particle measurements. Number concentration was highly correlated with the charge concentration, but the fit was different for solid particles versus all particles. This demonstrates that solid particles have a larger charge concentration than nucleation particles, which are included in the "all particles" case, and agrees with previous research showing that particles originating from inside the engine (solid particles) are more highly charged than particles formed when the exhaust dilutes (e.g., [22]), which have been found to carry little to no charges [37],

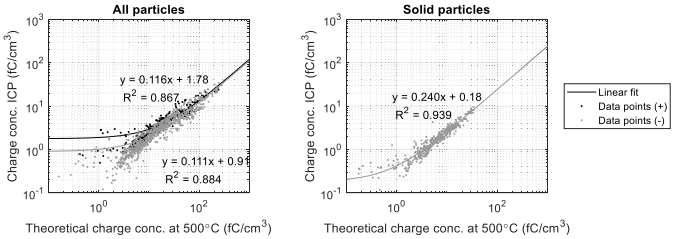


Fig. 5. Current measured with ICP compared to a theoretical current, calculated based on the data measured by the ELPI+ and assuming a Boltzmann charge distribution at 500 °C. The left plot shows the correlation for "all particle" test points, while the right plot shows solid particle test points. The data were averaged into 5-s sections from the original 1-Hz data and charge concentrations smaller than 0.1 fC/cm$^3$ were filtered out.

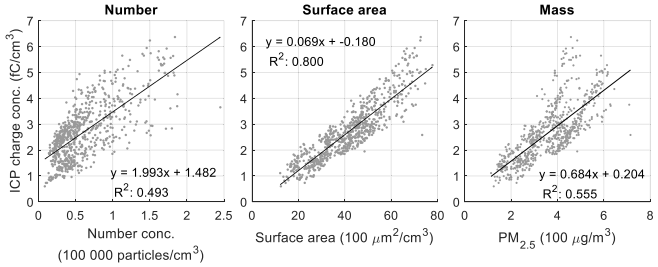


Fig. 6. Charge concentration measured with ICP compared to particle number and mass concentrations measured with ELPI+ during the ambient air measurement campaign. Each data point represents a 5-min average.

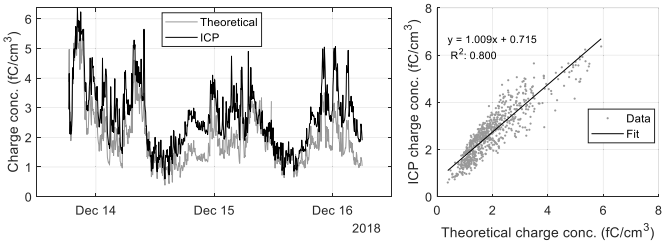


Fig. 7. Measured current from ambient charged particles, and the theoretical charge concentration calculated by assuming a Wiedensohler charge distribution and using ELPI+ size-distributed particle number concentration data. The data in both plots have been averaged into 5-min sections. Tick marks in the time series are placed at midnight.

[38]. When the aerosol is passed through the thermodenuder, not only are semivolatile particles removed, but solid particles that have been coated by the semivolatile vapors lose their coating, causing them to shrink. As a result, diffusional losses increase. Thus, some of the change in the charge concentration measured with the ICP can be due to higher diffusional losses in the sensor and in the sampling lines, and this effect is not corrected for. Selected time series for ICP current and number concentration are shown in Fig. S8 and time series for ELPI+ current and ICP current for each measurement point are shown in Fig. S9.

Finally, we looked at the charge concentration measured with ICP in comparison to a theoretical concentration derived from the ELPI+ number concentration and a Boltzmann charge distribution at 500 °C. This temperature was chosen based on previous findings that engine exhaust charge distributions match a Boltzmann equilibrium between 800 and 1100 K [18]. All the engine laboratory data are gathered in Fig. 5, which shows the linear fit between the measured current and theoretical charge concentration at 500 °C. The left side plot shows "all particles" cases and the right side plot shows "solid particles" cases. Note that the axes are logarithmic, which is why the linear fit function with a constant term looks nonlinear. In both cases, the correlation between the measured and theoretical charge concentration is very good ($R^2 > 0.8$), but the slope is far from one (0.12 for all particles and 0.24 for solid particles). Positive and negative polarities were not significantly different, which agrees with previous findings [18]. Examining the residuals for the "solid only" data points (Fig. S10) showed that larger CMD values (60–80 nm) were associated with positive residuals and vice versa for small CMD values (<20 nm).

### C. Ambient Roadside Measurements

The particle concentration during the roadside measurements was very high and ELPI+ showed signs of overloading, and thus, only the first few days of measurements after cleaning the ELPI+ are analyzed in depth. Many particle concentration metrics have been previously reported and are not repeated here [34].

To investigate the relationship of charge concentration to other particle metrics, Fig. 6 shows the correlation plots comparing the measurements with ICP to particle number, surface area, and mass ($PM_{2.5}$). The correlation was similar with number concentration ($R^2 = 0.493$) and mass concentration ($R^2 = 0.555$), while the correlation was highest with surface area ($R^2 = 0.800$).

Fig. 7 shows a time series of the electrical current measured with the ICP and a theoretical current calculated using the particle size distribution data measured with ELPI+ and Wiedensohler equation for the charge distribution at a temperature of 293.15 K or 20 °C. Along with the time series, the correlation between the two is displayed with a line fit to the data.

Fig. 7 shows that the ICP charge concentration is correlated with the theoretical charge concentration, and the difference between the two seems to be the smallest from midday to afternoon (tick marks are placed at midnight). The ICP charge concentration was larger than the theoretical at midnight. The fit line between the two for the whole duration is $y = 1.009x + 0.715$ with a correlation coefficient of $R^2 = 0.800$. We investigated the dependency of the residuals on the time of day, ambient temperature, electrometer temperature, particle size, and particle concentration (Fig. S11) and found that they depended on the time of day, ambient temperature, and particle size. Initially, we worried that the electrometer temperature might be the cause for residual dependence on ambient temperature, but the electrometer temperature had essentially no effect on the residuals. Instead, it seems that the particle size might be the root cause: smaller particles (<40 nm) resulted in negative residuals, while larger (~100 nm) particles resulted in positive residuals. Our interpretation is that when the particle

size distribution is dominated by small particles, they are either newly formed ambient particles or particles nucleated during fresh exhaust cooling and thus have no charge to begin with and have not reached charge equilibrium. Conversely, soot mode particles may still be closer to their initial higher charge, explaining the positive residual associated with them. The correlation coefficient between temperature and particle size was −0.34 (Table S3), which then explains why the ambient temperature seemed to affect the residuals: particle size was smaller and temperatures higher during midday to afternoon times. Surprisingly, hourly traffic counts (shown in Fig. S11) were unrelated to residuals.

We noted that the best fit line in Fig. 7 leaves a relatively large error for smaller values, and thus, we checked whether the analysis would change if the logarithmic values for measured and theoretical charge concentration were compared instead. While the fit improved for the smaller values, the interpretation of the residuals did not change.

## VI. Discussion

Comparing the charge concentration measured with ICP to other metrics revealed a high correlation ($R^2 > 0.7$) with number and surface area concentration in the engine laboratory measurements, whereas in the ambient measurement case, the correlation was equally good for number and mass ($R^2 \approx 0.5$) and the highest correlation was with surface area ($R^2 = 0.8$). The expectation was that the surface area would have the best correlation, as ion attachment is governed by Fuchs' surface area. The good agreement with mass concentration in the ambient measurement case was surprising and perhaps somewhat of a coincidence due to the specific aerosol properties at the location.

Previous engine exhaust studies have found particles to match a Boltzmann distribution of much higher temperatures than found here. For example, Maricq [18] observed that particles from a diesel passenger car corresponded to Boltzmann distributions at approximately 500 °C–800 °C. There are, however, a few differences between our studies: in our study, the vehicle was a heavy-duty truck, not a passenger car, and while we used a conventional CVS dilution system, Maricq used a "remote mix tee," which reduces the time from tailpipe to dilution tunnel. In the "All particles" case, the nucleation mode particles were at least partially responsible for the measured current being smaller than predicted, but when measuring only the solid particles, the measured charge concentration relative to the theoretical charge concentration only increased a little. Although the charge per particle (Table S2) is correlated with the CMD, $R^2 = 0.63$, we assume based on previous studies that the main reason for the change in the level of charge between the two cases is the removal of uncharged nucleation particles. The particle size distributions show that the solid particle measurements still included many small particles (Fig. S7). These must either be solid core particles [39], [40] or the thermodenuder was not efficient enough to remove all the semivolatile material. In future measurements, it would be interesting to measure particles directly from the tailpipe, or with less dilution, to see whether the charge per particle would better match previous findings.

In calculating a reference value for the measured ambient charge concentrations, we assumed that the particles had reached an equilibrium distribution described by the Wiedensohler equation. The measured charge concentration was slightly larger than the theoretical one, and we assumed that overcharged traffic-originated soot particles were the cause. When we aimed to verify this by analyzing the residuals of the fit to measured versus theoretical values, it turned out that traffic rates did not correlate with higher positive residuals (or negative residuals, for that matter), as is evident when comparing the hourly residuals to the traffic cycle in Fig. S11. From the analysis, we determined that particles in the soot mode size range were indeed more charged, but also nucleation particles were less charged than the equilibrium distribution predicted. Combustion engines can release particles from both modes, which is why the effect of traffic might be difficult to spot. In addition, other combustion sources nearby, such as cooking or heating, may also have contributed to the soot mode.

One aim of the engine and ambient measurements was to test the sensor performance in different settings and particle concentrations. The sensor's limit of detection is 1.636 fA, equal to three times the standard deviation of the electrometer signal when measuring clean air. This corresponds to a concentration of 4500 particles/cm$^3$ for 25-nm particles or 1500 particles/cm$^3$ of 100-nm particles with ambient charge levels. The ICP is, therefore, not a good choice for low particle concentrations. In the ambient measurements, the ICP was employed in a high-pollution environment for two weeks without problems (the data from these measurements were limited due to particle accumulation in the ELPI+), which shows that the geometry tolerates particle accumulation quite well. The highest currents we measured were around 700 fA, in the engine laboratory, but the electrometer can measure far larger currents (up to 400 000 fA); thus, high concentrations are not a problem.

The chosen mobility analyzer dimensions worked quite well in both environments. For these dimensions, many other applications are also possible, as the ICP can easily be modified for different needs by varying the collection voltage and/or flow rate. New versions with different dimensions could also be built to cater to specific needs. For instance, to target low concentrations, a higher flow rate could be used to increase the sensitivity (although the $Z_0$ value must be checked). Outside of modifying the mobility analyzer, particles in a soot mode size range could be better targeted by increasing the ion trap voltage, thereby removing more of the nucleation mode particles. Large particles with multiple charges could be removed aerodynamically before the sensor (with an impactor or a cyclone). Although we did use a cyclone in the ambient measurements here as well, the $dp_{50}$ was not sufficiently low to impact the measurements (2.2 $\mu$m).

We did not have an instrument available to measure the neutral particles penetrating the ICP in the ambient measurements. However, we examined this possibility by simulating the output of the ICP and a subsequent DC sensor (we used the $Pn$-curve for an eFilter) for different types of particle distributions. Two examples are shared in Fig. S12:

the first is an ambient number size distribution dominated by local emissions and the second is dominated by more aged emissions in the accumulation mode. Assuming that the nucleation and accumulation mode particles have reached an equilibrium state (calculated for negative particles from the empirical Wiedensohler equation [15]) and a Boltzmann distribution at 800 K for the soot mode particles, the IC to DC ratio was 50% for the first case and 30% for the second case. Therefore, this combination of sensors could be used to detect local traffic emissions based on this ratio, but as was seen in the ambient measurements, nucleation mode particles had less inherent charge than in theoretical equilibrium conditions.

## VII. Conclusion

In this article, we presented a new electrical sensor type and showed it to be suitable for measuring particles both in an engine laboratory and in ambient measurements in a polluted environment. When used in tandem with other instruments, such as we did here with the ELPI+, it can give information of the charge state of the aerosol. Compared to most previous electrical sensors, the benefit of the ICP is that a charging mechanism, often vulnerable to contamination, is not needed, whereas the downside of the ICP-sensor is that larger particle concentrations are required to produce a detectable current than in DC sensors.

## Acknowledgment

The authors would like to thank Matthew Bloss for helping with the ambient measurements and Indian Oil Corporation Ltd., Faridabad (IOCL), for providing the facilities for the engine laboratory tests and operating the engine dynamometer, and for providing the mobile laboratory to house instruments during the ambient campaign.

## References

[1] U. Lohmann and J. Feichter, "Global indirect aerosol effects: A review," *Atmos. Chem. Phys.*, vol. 4, no. 6, pp. 7561–7614, 2004, doi: 10.5194/acpd-4-7561-2004.

[2] M. O. Andreae, C. D. Jones, and P. M. Cox, "Strong present-day aerosol cooling implies a hot future," *Nature*, vol. 435, pp. 1187–1190, Jun. 2005, doi: 10.1038/nature03671.

[3] J. Lelieveld, J. S. Evans, M. Fnais, D. Giannadaki, and A. Pozzer, "The contribution of outdoor air pollution sources to premature mortality on a global scale," *Nature*, vol. 525, no. 7569, pp. 367–371, 2015, doi: 10.1038/nature15371.

[4] *Spreading Like Wildfire—The Rising Threat of Extraordinary Landscape Fires*, United Nations Environment Programme, Nairobi, Kenya, 2022.

[5] P. Kulkarni and P. A. Baron, "An approach to performing aerosol measurements," in *Aerosol Measurement: Principles, Techniques, and Applications*, 3rd ed., P. Kulkarni, K. Willeke, and P. A. Baron, Eds. 2011, pp. 55–65.

[6] J. J. Caubel, T. E. Cados, C. V. Preble, and T. W. Kirchstetter, "A distributed network of 100 black carbon sensors for 100 days of air quality monitoring in west Oakland, California," *Environ. Sci. Technol.*, vol. 53, no. 13, pp. 7564–7573, Jul. 2019, doi: 10.1021/acs.est.9b00282.

[7] M. Fierz, D. Meier, P. Steigmeier, and H. Burtscher, "Aerosol measurement by induced currents," *Aerosol Sci. Technol.*, vol. 48, no. 4, pp. 350–357, Apr. 2014, doi: 10.1080/02786826.2013.875981.

[8] J. Kuula et al., "Long-term sensor measurements of lung deposited surface area of particulate matter emitted from local vehicular and residential wood combustion sources," *Aerosol Sci. Technol.*, vol. 54, no. 2, pp. 190–202, Feb. 2020, doi: 10.1080/02786826.2019.1668909.

[9] W. C. Hinds, *Aerosol Technology: Properties, Behavior, and Measurement of Airborne Particles*, 2nd ed. New York, NY, USA: Wiley, 1999.

[10] R. T. Nishida, T. J. Johnson, J. S. Hassim, B. M. Graves, A. M. Boies, and S. Hochgreb, "A simple method for measuring fine-to-ultrafine aerosols using bipolar charge equilibrium," *ACS Sensors*, vol. 5, no. 2, pp. 447–453, Feb. 2020, doi: 10.1021/acssensors.9b02143.

[11] S. Jakubiak and P. Oberbek, "Determination of the concentration of ultrafine aerosol using an ionization sensor," *Nanomaterials*, vol. 11, no. 6, p. 1625, Jun. 2021, doi: 10.3390/nano11061625.

[12] D. Bilby, D. J. Kubinski, and M. M. Maricq, "Current amplification in an electrostatic trap by soot dendrite growth and fragmentation: Application to soot sensors," *J. Aerosol Sci.*, vol. 98, pp. 41–58, Aug. 2016, doi: 10.1016/j.jaerosci.2016.03.003.

[13] P. Eastwood, *Particle Emissions From Motor Vehicles*. Hoboken, NJ, USA: Wiley, 2008.

[14] D. Keefe, P. Nolan, and T. Rich, "Charge equilibrium in aerosols according to the Boltzmann law," *Proc. Roy. Irish Acad. Sect. A, Math. Phys. Sci.*, vol. 60, pp. 27–45, Jul. 1959.

[15] A. Wiedensohler, "An approximation of the bipolar charge distribution for particles in the submicron size range," *J. Aerosol Sci.*, vol. 19, no. 3, pp. 387–389, Jun. 1988, doi: 10.1016/0021-8502(88)90278-9.

[16] P. Kulkarni, P. A. Baron, and K. Willeke, *Aerosol Measurement: Principles, Techniques, and Applications*. Hoboken, NJ, USA: Wiley, 2011.

[17] H. Burtscher, A. Reis, and A. Schmidt-Ott, "Particle charge in combustion aerosols," *J. Aerosol Sci.*, vol. 17, no. 1, pp. 47–51, Jan. 1986.

[18] M. M. Maricq, "On the electrical charge of motor vehicle exhaust particles," *J. Aerosol Sci.*, vol. 37, no. 7, pp. 858–874, Jul. 2006, doi: 10.1016/j.jaerosci.2005.08.003.

[19] V. Jokinen, *Aerosolinhiukkasten Ja Ilman Ionien Mittaus Differentiaalisella Liikkuvuusanalysaatorilla*. Helsinki: Aerositutkimusseura, 1995.

[20] E. R. Jayaratne, X. Ling, and L. Morawska, "Observation of ions and particles near busy roads using a neutral cluster and air ion spectrometer (NAIS)," *Atmos. Environ.*, vol. 84, pp. 198–203, Feb. 2014, doi: 10.1016/j.atmosenv.2013.11.045.

[21] D. B. Kittelson and D. Y. H. Pui, "Electrostatic collection of diesel particles," *SAE Trans.*, vol. 95, no. 1, pp. 51–62, 1986.

[22] T. Lähde et al., "Heavy duty diesel engine exhaust aerosol particle and ion measurements," *Environ. Sci. Technol.*, vol. 43, no. 1, pp. 163–168, 2009, doi: 10.1021/es801690h.

[23] E. R. Jayaratne, X. Ling, and L. Morawska, "Comparison of charged nanoparticle concentrations near busy roads and overhead high-voltage power lines," *Sci. Total Environ.*, vol. 526, pp. 14–18, Sep. 2015, doi: 10.1016/j.scitotenv.2015.04.074.

[24] E. S. Lee, B. Xu, and Y. Zhu, "Measurements of ultrafine particles carrying different number of charges in on- and near-freeway environments," *Atmos. Environ.*, vol. 60, pp. 564–572, Dec. 2012, doi: 10.1016/j.atmosenv.2012.06.085.

[25] J. Alanen et al., "The formation and physical properties of the particle emissions from a natural gas engine," *Fuel*, vol. 162, pp. 155–161, Dec. 2015, doi: 10.1016/j.fuel.2015.09.003.

[26] F. Mylläri et al., "Physical and chemical characteristics of flue-gas particles in a large pulverized fuel-fired power plant boiler during co-combustion of coal and wood pellets," *Combustion Flame*, vol. 176, pp. 554–566, Feb. 2017, doi: 10.1016/j.combustflame.2016.10.027.

[27] L. Stabile, E. R. Jayaratne, G. Buonanno, and L. Morawska, "Charged particles and cluster ions produced during cooking activities," *Sci. Total Environ.*, vols. 497–498, pp. 516–526, Nov. 2014, doi: 10.1016/j.scitotenv.2014.08.011.

[28] A. Järvinen, M. Aitomaa, A. Rostedt, J. Keskinen, and J. Yli-Ojanperä, "Calibration of the new electrical low pressure impactor (ELPI+)," *J. Aerosol Sci.*, vol. 69, pp. 150–159, Mar. 2014, doi: 10.1016/J.JAEROSCI.2013.12.006.

[29] H. Tammet, *The Aspiration Method for the Determination of Atmospheric-Ion Spectra*, vols. 195–2. Jerusalem: Israel Program for Scientific Translations, 1970.

[30] J. Yli-Ojanperä, J. M. Mäkelä, M. Marjamäki, A. Rostedt, and J. Keskinen, "Towards traceable particle number concentration standard: Single charged aerosol reference (SCAR)," *J. Aerosol Sci.*, vol. 41, no. 8, pp. 719–728, Aug. 2010, doi: 10.1016/j.jaerosci.2010.04.012.

[31] S. Martikainen et al., "Reducing particle emissions of heavy-duty diesel vehicles in India: Combined effects of diesel, biodiesel and lubricating oil," *Atmos. Environ., X*, 2023, Art. no. 100202, doi: 10.1016/j.aeaoa.2023.100202.

[32] J. Keskinen, K. Pietarinen, and M. Lehtimäki, "Electrical low pressure impactor," *J. Aerosol Sci.*, vol. 23, no. 4, pp. 353–360, 1992.

[33] L. Salo et al., "Emission measurements with gravimetric impactors and electrical devices: An aerosol instrument comparison," *Aerosol Sci. Technol.*, vol. 53, no. 5, pp. 526–539, May 2019, doi: 10.1080/02786826.2019.1578858.
[34] L. Salo et al., "The characteristics and size of lung-depositing particles vary significantly between high and low pollution traffic environments," *Atmos. Environ.*, vol. 255, Jun. 2021, Art. no. 118421, doi: 10.1016/j.atmosenv.2021.118421.
[35] P. G. Gormley and M. Kennedy, "Diffusion from a stream flowing through a cylindrical tube," *Proc. Roy. Irish Acad. Sect. A, Math. Phys. Sci.*, vol. 52, pp. 163–169, Sep. 1948. [Online]. Available: http://www.jstor.org/stable/20488498
[36] Y.-S. Cheng, "Instruments and samplers based on diffusional separation," in *Aerosol Measurement: Principles, Techniques, and Applications*, 3rd ed., P. Kulkarni, K. Willeke, and P. A. Baron, Eds. 2011, pp. 365–379.
[37] H. Jung and D. B. Kittelson, "Measurement of electrical charge on diesel particles," *Aerosol Sci. Technol.*, vol. 39, no. 12, pp. 1129–1135, Dec. 2005.
[38] H. Ma, H. Jung, and D. B. Kittelson, "Investigation of diesel nanoparticle nucleation mechanisms," *Aerosol Sci. Technol.*, vol. 42, no. 5, pp. 335–342, Mar. 2008.
[39] T. Rönkkö, A. Virtanen, J. Kannosto, J. Keskinen, M. Lappi, and L. Pirjola, "Nucleation mode particles with a nonvolatile core in the exhaust of a heavy duty diesel vehicle," *Environ. Sci. Technol.*, vol. 41, no. 18, pp. 6384–6389, Sep. 2007, doi: 10.1021/es0705339.
[40] A. D. Filippo and M. M. Maricq, "Diesel nucleation mode particles: Semivolatile or solid?" *Environ. Sci. Technol.*, vol. 42, no. 21, pp. 7957–7962, Nov. 2008, doi: 10.1021/es8010332.

**Laura Salo** is pursuing the Ph.D. degree in aerosol physics with Tampere University, Tampere, Finland.

She is with the Aerosol Physics Laboratory, Faculty of Engineering and Natural Sciences, Tampere University. She began her studies in 2017 and since has been involved with air quality, aerosol emissions, and instrument development.

**Antti Rostedt** is a Staff Scientist with the Aerosol Physics Laboratory, Faculty of Engineering and Natural Sciences, Tampere University, Tampere, Finland. His main research interests are aerosol measurement technology and instrument development.

**Heino Kuuluvainen** was born in Hämeenlinna, Finland, in 1985.

He currently works as a University Instructor in Physics and is involved in aerosol physics research with the Aerosol Physics Laboratory, Faculty of Engineering and Natural Sciences, Tampere University, Tampere, Finland. His research interests include surface interaction of aerosol particles, urban air quality, and particulate emissions.

**Kimmo Teinilä** is working as a Senior Research Scientist at the Aerosol Composition Research Group, Finnish Meteorological Institute, Helsinki, Finland. His research interests include ambient aerosol measurements, especially particle chemical composition measurements.

**Rakesh K. Hooda** is a Senior Scientist and the Coordinator of Indo-Finnish Research at the Aerosol Composition research Group, Finnish Meteorological Institute, Helsinki, Finland. He works for the last 20 years on aerosols' physicochemical and optical properties; quantifying sources and emission inventories; boundary layer dynamics, atmospheric aging, and transformation due to physicochemical processes; direct, semidirect, and indirect effect studies of aerosol; and particle climate and health impacts.

**Md. Hafizur Rahman** received the M.Tech. degree in environmental biotechnology from Jadavpur University, Kolkata, India, in 2017.

He is one of the research professionals at The Energy and Resources Institute (TERI), New Delhi, India. His research interests include air quality monitoring and assessment, development of air pollutant emission inventory, and developing innovative solutions for air quality management.

**Arindam Datta** received the Ph.D. degree in environmental sciences from the University of Kalyani, Kalyani, India, in 2008.

He was a Fulbright Fellow at the Ohio State University, Columbus, OH, USA, and a Postdoctoral Research Fellow at the University of Aberdeen, Aberdeen, U.K. He is one of the senior professionals at The Energy and Resources Institute (TERI), New Delhi, India. His research interests include sector-specific air pollution and GHG emission inventory and emission factor development.

**Ved Prakash Sharma** has more than 24 years of experience in environmental management, on air quality management monitoring, laboratory analysis, including black carbon monitoring in association with the Finnish metrological institute. He was responsible for aerosol monitoring center in the central Himalayas from 2005 to 2018. His other areas of expertise are in monitoring biomass heat exposure, workplace exposure, water quality and wastewater quality, solid waste characteristics, and OSHA auditing. He is the Laboratory Head of the Air Quality Laboratory and the Radiological Safety officer (RSO) of The Energy and Resources Institute (TERI), New Delhi, India, responsible for nucleonic Gauge facility of the aerosol monitoring instruments. He has published about 25 research papers in various international and national journals.

**Sanjukta Subudhi** received the Ph.D. degree from the University of Delhi, New Delhi, India, in 2001.

She was a Postdoctorate at the National Center for Genetic Engineering and Biotechnology, National Science and Technology Development Agency (NSTDA), Bangkok, Thailand. She is a Senior Scientist and the Group Leader at the Microbial Biofuels and Biochemical Group, The Energy and Resources Institute (TERI), New Delhi. Her subject domain spans technology development and demonstration for production of biofuels (gaseous and liquid biofuels: biohydrogen, bioethanol, biodiesel, and biomethane) and value-added industry platform biochemical, including high-value biopigments, in a biorefinery approach through microbial interventions.

**Antti Hyvärinen** is the Head of the Atmospheric Composition Research Unit, Finnish Meteorological Institute, Helsinki, Finland. His expertise lies in measurements of aerosol properties in various field environments around global hotspots for aerosol research, including India.

**Hilkka Timonen** is a Senior Scientist and a Leader of the Aerosol Composition Research Group, Finnish Meteorological Institute, Helsinki, Finland. She has long-term experience on chemical and physical characterization of ambient aerosol as well as emissions originating from different anthropogenic emission sources.

**Eija Asmi** received the Ph.D. degree in aerosol physics from the University of Helsinki, Helsinki, Finland, in 2010.

She has been a Senior Scientist and the Head of the Group Aerosols and Climate, Finnish Meteorological Institute, Helsinki, since 2008. Her main research interests are aerosol particle climate impacts. She is a specialist on in situ experimental studies of absorbing aerosols and aerosol–cloud interactions.

**Sampsa Martikainen** is pursuing the Ph.D. degree with the Aerosol Physics Laboratory, Faculty of Engineering and Natural Sciences, Tampere University, Helsinki, Finland.

His research is on engine emissions, focusing especially on the smallest particles.

**Panu Karjalainen** is a Senior Research Fellow at the Institute for Advanced Study and the Aerosol Physics Laboratory, Faculty of Engineering and Natural Sciences, Tampere University, Helsinki, Finland. His experimental research focuses on aerosol measurement method development and in-depth characterization of emission aerosols.

**Banwari Lal** is currently heading the Environmental and Industrial Biotechnology Division in the capacity of Senior Director at The Energy and Resources Institute (TERI), New Delhi, India. He is also the Managing Director at ONGC TERI Biotech Ltd (OTBL), New Delhi, a joint venture of ONGC and TERI. He is having more than 35 years of research experience in the field of petroleum biotechnology. He has developed three technologies, namely, “oilzapper (for bioremediation of oil spill),” “microbial enhanced oil recovery,” and “prevention of paraffin deposition in oil well tubing and flow lines.” All the three technologies are patented and commercialized.

**Jorma Keskinen** is the Head of the Aerosol Physics Laboratory, Faculty of Engineering and Natural Sciences, Tampere University, Helsinki, Finland. His research interests cover aerosol measurement techniques, emissions of engines, vehicles, and ships—especially nanoparticles, volatility, and secondary aerosol formation potential.

**Topi Rönkkö** is the Leader of the Aerosol Emissions and Air Quality Research Group, Aerosol Physics Laboratory, Faculty of Engineering and Natural Sciences, Tampere University, Helsinki, Finland. His research focuses on particle emissions from anthropogenic sources and their effects on air quality, human health, and climate.